Journal of Maps

ISSN: (Print) (Online) Journal homepage: www.tandfonline.com/journals/tjom20

Geology of the Late Carboniferous, Permian and Early Triassic basins of the Eastern Pyrenees

Josep Gisbert, Ana Simón-Muzás, Antonio Casas-Sainz & Ruth Soto

To cite this article: Josep Gisbert, Ana Simón-Muzás, Antonio Casas-Sainz & Ruth Soto (2024) Geology of the Late Carboniferous, Permian and Early Triassic basins of the Eastern Pyrenees, Journal of Maps, 20:1, 2321382, DOI: 10.1080/17445647.2024.2321382

To link to this article: https://doi.org/10.1080/17445647.2024.2321382

JOURNAL OF MAPS
2024, VOL. 20, NO. 1, 2321382
https://doi.org/10.1080/17445647.2024.2321382

SCIENCE

OPEN ACCESS Check for updates

Geology of the Late Carboniferous, Permian and Early Triassic basins of the Eastern Pyrenees

Josep Gisbert [a], Ana Simón-Muzás [a], Antonio Casas-Sainz [a] and Ruth Soto [b]

[a]Departamento de Ciencias de la Tierra, Geotransfer-IUCA, Universidad de Zaragoza, Zaragoza, Spain; [b]Instituto Geológico y Minero de España (IGME), CSIC, Unidad de Zaragoza, Zaragoza, Spain

ABSTRACT

We present a detailed geological map of the Upper Carboniferous, Permian and Triassic rocks of the southern border of the Axial Zone in the Eastern Pyrenees. These units were deposited in three intra-mountain, terrestrial basins, characterized by the emplacement/deposition of volcanic, sub-volcanic and volcaniclastic units (ca. 1000 m thick) together with continental red beds. The map is based on unpublished drafts, sketches and structural data. This previous information was complemented with new structural, petrologic and stratigraphic data. The geological map is presented together with three cross-sections, a detailed lithological description, and a stratigraphic correlation panel to help understand the stratigraphy, volcanism and structure and, ultimately, the geometry and origin of the highly subsident areas of this segment of the chain in post-Variscan times. The geological map gives new clues for reconstructing the geometry of these basins and the distribution of the volcanic episodes during the Late Carboniferous and Permian.

ARTICLE HISTORY
Received 26 October 2023
Revised 8 February 2024
Accepted 15 February 2024

KEYWORDS
Late Carboniferous; Permian; Triassic; Volcanism; Pyrenees; Axial Zone

1. Introduction

The Pyrenees is one of the most studied mountain chain worldwide, and numerous maps synthesize its overall geology (mainly made by ICGC, Institut Cartogràfic i Geològic de Catalunya; see also Ternet et al., 2008; 1:250,000), large-scale structures (Choukroune & Séguret, 1973), stratigraphy (Soler i Sampere et al., 1972), paleomagnetic data (López Berdonces et al., 2008; Porquet et al., 2017) or rather deal with the particular features of specific areas (Puigdefábregas, 1975; Rodríguez-Méndez et al., 2013). In spite of this large amount of information, the southern sector of the Axial Zone in the Eastern Pyrenees is shown with low level of detail in many published geological maps. This is mainly due to the presence of Upper Carboniferous-Permian volcaniclastic and volcanic rocks. These rocks, because of their sharing characteristics sedimentary and igneous features altogether, require a thorough understanding of their original mineralogy, facies arrangement and stratigraphic frame (Gisbert, 1981; Martí, 1986) in order to be correctly mapped. These Upper Carboniferous and Permian units were deposited in a series of sedimentary basins that can be recognized along the southern margin of the Axial Zone. These basins are, from west to east, the Erillcastell-Estac, Cadí and Castellar de n'Hug basins, and they constitute key areas (due to their good exposure, lithological variety and thickness of series) to understand the volcanic episodes linked to the late Paleozoic break-up of Pangea and its geodynamic consequences. Precisely, the present-day Pyrenean zone is one of the weakness zones along which the supercontinent broke apart during Permian through Cretaceous times (Soto et al., 2019).

The main objective of this work is to help understand the stratigraphy, volcanism and structure of the Late Carboniferous-Triassic Erillcastell-Estac, Cadí and Castellar de n'Hug basins in the frame of the Eastern Pyrenees, in order to establish a reliable frame to define consistent basin models for this particularly interesting stage of Earth's history. To this aim, we present: (1) a detailed lithological description of these units deposited during the late-orogenic to post-orogenic period of the Variscan orogeny in the southeastern Pyrenees; (2) a cartography (originally at 1: 25,000 scale) of the different lithologies corresponding to the different stages, showing their lateral facies changes; and (3) a high-resolution cartography of fractures and faults, together with 641 bedding data that allow us to define the structural architecture of the study area. Some of the information collected during the 70s and 80s is very valuable due to the impossibility of its current acquisition because of the growth of the vegetation canopy during the last three decades linked to the reduction of extensive

CONTACT Ruth Soto r.soto@igme.es Instituto Geológico y Minero de España (IGME), CSIC, Unidad de Zaragoza, Zaragoza 50059, Spain
Supplemental data for this article can be accessed online at https://doi.org/10.1080/17445647.2024.2321382.

livestock farming. The cartographic relationships between the Upper Carboniferous, Permian and Triassic units are presented in a geo-referenced map attached to this article.

2. Location and geological settings

The study area covers the outcrops of the Upper Carboniferous, Permian and Triassic materials of the southern border of the Axial Zone in the Eastern Pyrenees, totaling a length of nearly 150 km along an E-W direction.

The Pyrenees are a WNW-ESE trending, asymmetric, doubly-vergent orogen with a dominant southwards vergence. They are limited by the Aquitaine and Ebro foreland basins to the north and south, respectively (Figure 1) and by the Mediterranean Sea and the Atlantic Ocean eastwards and westwards, respectively. The Pyrenees are commonly subdivided from north to south into the North Pyrenean Zone, the Axial Zone and the South Pyrenean Zone (Mattauer, 1968). Mesozoic and Cenozoic rocks dominate in the North- and South-Pyrenean Zones, and it is in the Axial Zone where the Paleozoic rocks, that constitute the basement of the chain, crop out. Rocks belonging to the Axial Zone have experimented the effects of two different orogenic processes: the Variscan orogeny during Carboniferous time (Barnolas & Pujalte, 2004) and the Alpine orogeny during the Late Cretaceous-Cenozoic time interval (Muñoz, 1992; Vergés et al., 2002). These orogenic processes post-date two rift-post-rift cycles during the Paleozoic and the Mesozoic. Structures related to these stages are often preserved, but sometimes they are difficult to interpret because of the superposition of extensional and compressional features along the geological evolution. The present-day structure and topography of the chain is mainly the result of the Cenozoic Pyrenean compression, that generated an antiformal stack made up of several thrust sheets mainly composed of Paleozoic rocks. In the Eastern Pyrenees these thrust sheets are named, from bottom to top, Rialp, Orri, Erta and Nogueres (Muñoz, 1992). The dominant transport direction of thrust sheets is toward the SSW (Saura & Teixell, 2006). The Paleozoic rocks were affected during the Late Carboniferous-Permian time by volcanic episodes linked to Late-Variscan, crustal- or lithospheric-scale faults along which magma ascent took place. These faults are found throughout Iberia (Aldega et al., 2019 and references therein, Arthaud & Matte, 1977; López-Gómez et al., 2019), and show several directional maxima (NW-SE, NE-SW and E-W). During the post-Variscan period, small intra-mountainous basins were originated and filled with volcanic and sedimentary rocks (Gisbert, 1986). Subsequently, during the Pyrenean compression, most of these basins were inverted and/or transported southwards in the hanging wall of some of the above-mentioned basement thrust sheets (e.g. the Cadí, Erillcastell-Estac basins in the Orri thrust sheet).

A detailed description of the stratigraphy of the Upper Carboniferous-Permian volcanic and sedimentary rocks appears in section 4.1, following Gisbert's (1981) work.

3. Materials and methods

3.1. Original unreleased material

The cartography presented in this work is mainly based on drafts, sketches, structural data and detailed unpublished maps carried out in the study area during the 70s and 80s by Josep Gisbert and co-workers. Only the cartography of the easternmost zone was included in Gisbert (1981).

The cartographies and data used are listed below.

- Sketch map (Figure 2(1)) of the Late Carboniferous-Permian Cadí basin in scale 1:20,000 based on information collected directly on the field and aerial photograph interpretation (black and white photographs in scale 1:33,000 of the Geographic Service of the Spanish Army, flights 1960–1970). The geological information was plotted on a delineated topographic map in scale 1:25,000.
- Detailed geological map in scale 1:25,000 (Figure 2 (2)) of the Upper Carboniferous, Permian and Triassic units located in the study area. Gisbert and co-workers carried out this work between 1979 to 1984 on a delineated topographic map in scale 1:20,000.
- Bedding attitude dataset georeferenced on a topographic base map.

3.2. Cartography georeferencing and digitization

The workflow to digitize and georeferencing all the above mentioned data followed three steps: (1) scanning of data in high resolution, jpg format, (2) georeferencing the scanned data using the georeferencing tool available on *QGIS Desktop 3.30.1 software* (available online at https://qgis.org), and (3) elaboration of the final digitized cartography.

The georeferencing of the different maps was done using topographic map sheets downloaded from the IGN (Instituto Geográfico Nacional, official website: https://centrodedescargas.cnig.es/CentroDescargas/index.jsp) in scale 1:25,000 (MTN25 raster, time zone 31 UTM) and in a Cloud Optimized GeoTIFF format. The reference coordinate geographic system used was ETRS89/UTM zone 31 EPSG: 25831. The

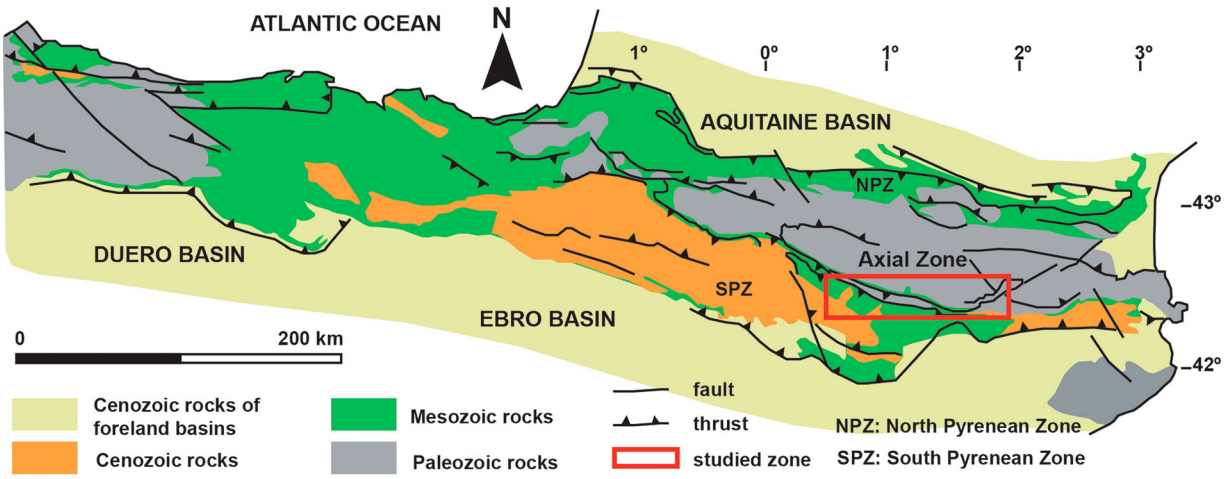

Figure 1. Location of the mapped zone (squared in red) in the Pyrenees (modified from Izquierdo-Llavall et al., 2013).

georeferencing tool in the QGIS software allows to georeference a raster or an image file by assigning it equivalent and characteristic points also appearing in equivalent georeferenced documents or maps (i.e. topographic maps). The digitization (Figure 2(3)) was done directly on the georeferenced scanned maps tracing the contact lines between units, structural elements (i.e. faults) and geographic elements (villages and hamlets). In the last step, the map was converted to a vector file with Inkscape (1.2.2 and 1.3 versions) software.

3.3. Revision and elaboration of the final cartography

Historical and recent orthophotos were consulted to check the stratigraphic contacts between units and the main fault traces. Orthophotos were downloaded from the IGN (Instituto Geográfico Nacional, official website: https://centrodedescargas.cnig.es/CentroDescargas/index.jsp) in scales 1: 50,000 and 1: 25,000, ETRS89 in a COG or ECW format. Structural data acquired in the field specifically for this work were also added and some of the contacts were slightly corrected after field inspection.

4. Results

The resulting geological map represents a new product showing much more resolution and detailed information than previous works done in the studied area. Moreover, it shows lithological changes of several stratigraphic units that represent indispensable information to better understand the Late Carboniferous-Permian geodynamic evolution and volcanism in the Pyrenean chain.

According to their facies distribution, thickness changes and/or structural patterns, three Late Carboniferous-Permian basins can be distinguished in the mapped area: (1) Erillcastell-Estac (also known as Malpàs-Sort), (2) Cadí and (3) Castellar de n'Hug. They have traditionally received the name of nearby villages (e.g. Erillcastell, Malpàs, Estac or Sort) or remarkable topographic features (e.g. Cadí Range). The Late Carboniferous-Permian Ogassa basin, located farther east, is not included in the study area. In order to avoid confusion, the different basins are referred to with their most common names.

4.1. Stratigraphy

The stratigraphic units distinguished on the main map are (i) pre-Variscan basement rocks, (ii) post-Variscan, Upper Carboniferous-Permian lithostratigraphic units, and (iii) Triassic rocks. The pre-Variscan basement rocks are constituted by units deposited before the Variscan orogeny, which took place during the Early Carboniferous. They include Cambro-Ordovician shales and sandstones, Ordovician conglomerates, quartzites, shales and greywackes, Silurian black shales, Devonian limestones, marls and shales and Lower Carboniferous conglomerates, sandstones and shales (Sanz-López, 2004). The post-Variscan Upper Carboniferous-Permian lithostratigraphic units in the Pyrenees were originally defined by Gisbert (1981) in the Cadí basin. In the study area, these lithostratigraphic units can be also followed in the Erillcastell-Estac and Castellar de n'Hug basins (Figure 3). The along-strike thickness variations, lateral continuity and stratigraphic boundaries of these units between the three studied basins are shown in the correlation panel (Supplementary material), that shows thickness data obtained from their detailed mapping. Figure 4 shows a synthetic lithological sketch where the units defined by Gisbert (1981) are correlated with the formations and volcanic episodes proposed by other authors.

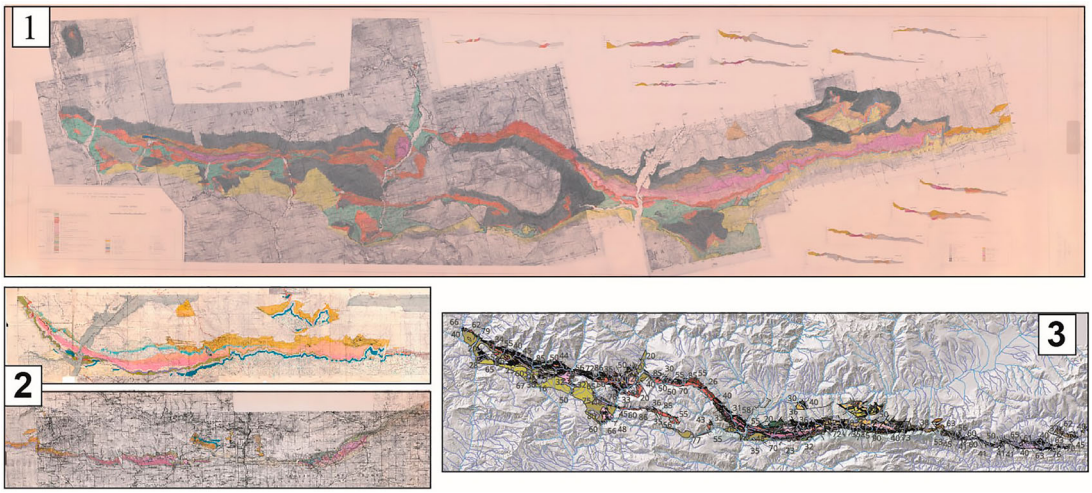

Figure 2. Original cartographies and sketches (Gisbert, 1981 and unpublished documents by this author): (1) General cartography of the studied zone (1 × 1 km orthogonal grid), (2) detailed sketches from the Cadí basin and Castellar de n'Hug zone (1 × 1 km orthogonal grid). (3) Digitization carried out in the present work.

A brief description of the Upper Carboniferous, Permian and Triassic units is presented here following Gisbert (1981). This detailed description in each unit allows us to recognize the above-mentioned stratigraphic features related to lateral facies variations necessary to constrain the evolution of these basins.

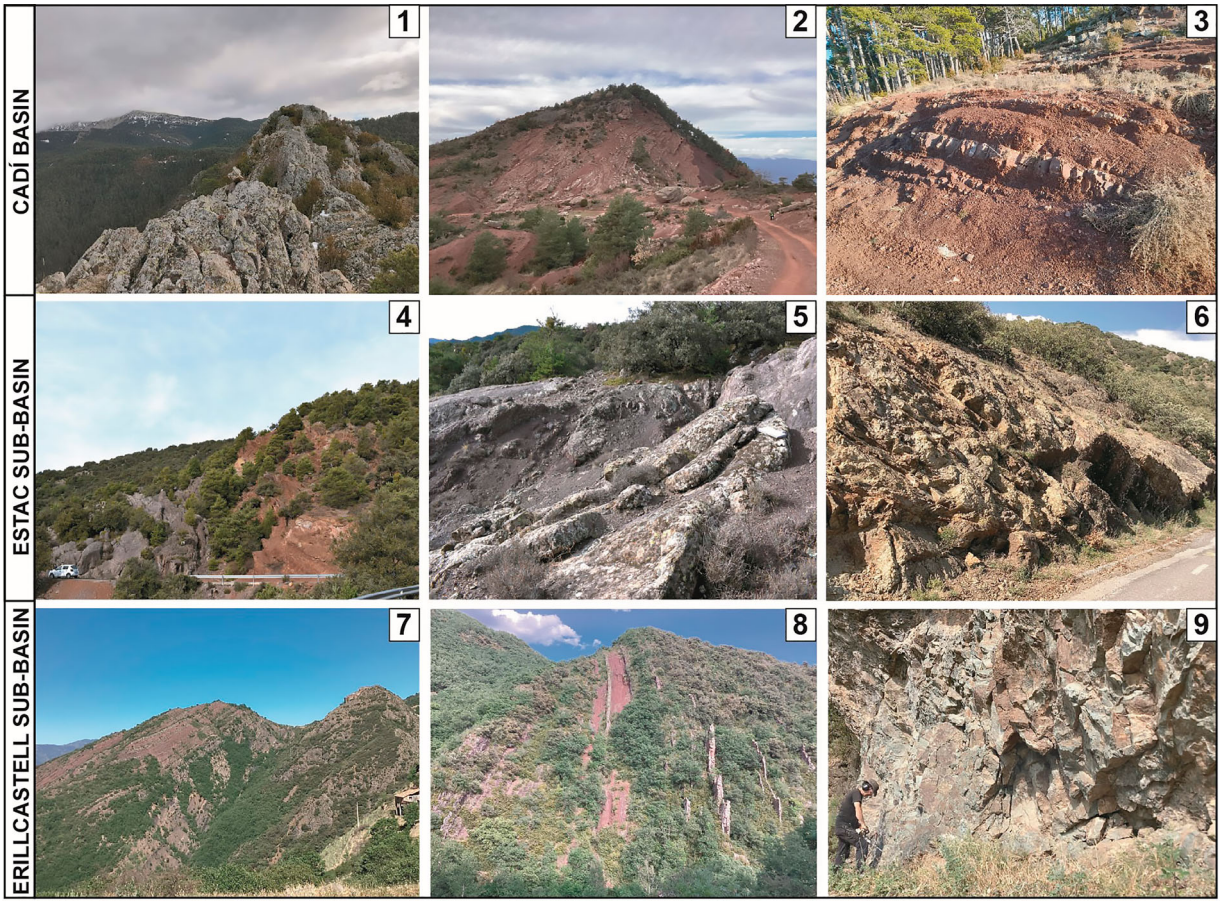

Figure 3. Different views of the landscapes and outcrops from the Cadí basin, Estac and Erillcastell sub-basins: (1) Andesitic intrusive body in the foreground. The Cadí Range at the background; (2) General view of the red bed succession (LRU and URU); (3) Detail of an outcrop of the LRU: an alternation of reddish siltstones, shales and sandstones is observed; (4) General view that shows the limit between the lava flows (left) and the red bed succession (right); (5) Detail of an outcrop of the volcanic lava flows of the upper GU; (6) Detail of an outcrop of the volcanic lava flows of the lower GU; (7) General view of the red bed succession (left) and the lava flows (right) next to the Peranera hamlet. (8) Close-up view of the red bed succession showing vertical bedding where the sandstone levels stand above the forest; (9) Detail of a lava flow outcrop.

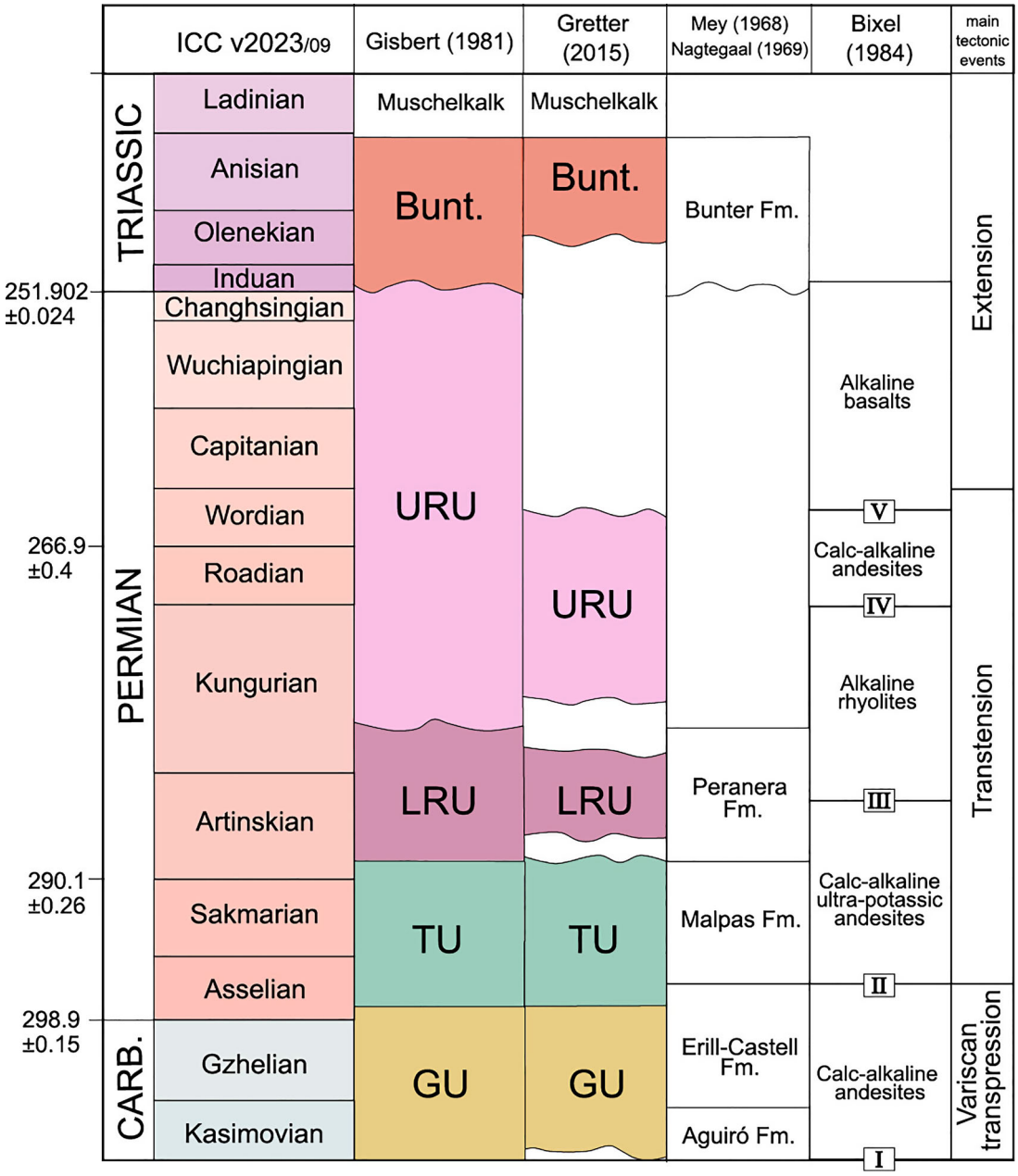

Figure 4. Synthetic lithostratigraphic sketch that correlates the units defined by Gisbert (1981) with the formations, ages and volcanic episodes proposed by other authors (modified from López-Gómez et al., 2019).

- Gray Unit (GU). This unit is composed of detrital (breccias, conglomerates and sandstones) and lacustrine (laminated shales and coal) sediments and volcanic rocks. Volcanic rocks are composed by cinerites, volcanic tuffs, ignimbrites, volcanic agglomerates and andesitic lava flows whose combined thicknesses range between 20 and 130 m in the central area. Toward the top of the unit, there are volcanic tuffs with more acidic composition. The GU is considered Stephanian B and part of Stephanian C according to the paleoflora studies carried in the lacustrine sediments (Gisbert, 1981). Recent absolute dating of rocks of this unit from the Castellar de n'Hug basin indicates an Ordovician age (Martí et al., 2019). However, more studies would be needed to better constrain their age and/or to validate the lateral correlation between these rocks in the Cadí and Castellar de n'Hug basins.
- Transition Unit (TU). This unit crops out in the western half of the Cadí basin. It appears in paraconformity or low-angle unconformity with the overlying unit and disappears toward the east due to a lateral pinchout of the volcanic rocks. It consists of conglomerates, alternating greenish and gray sandstones, shales and coal with intercalations of red and greenish ignimbrites and volcanic tuffs. The detrital deposits are arranged in fining-upwards megasequences topped by lacustrine limestones or shales with calcified anhydrite nodules. The Carboniferous-Permian limit is located within this unit (Gisbert, 1981).

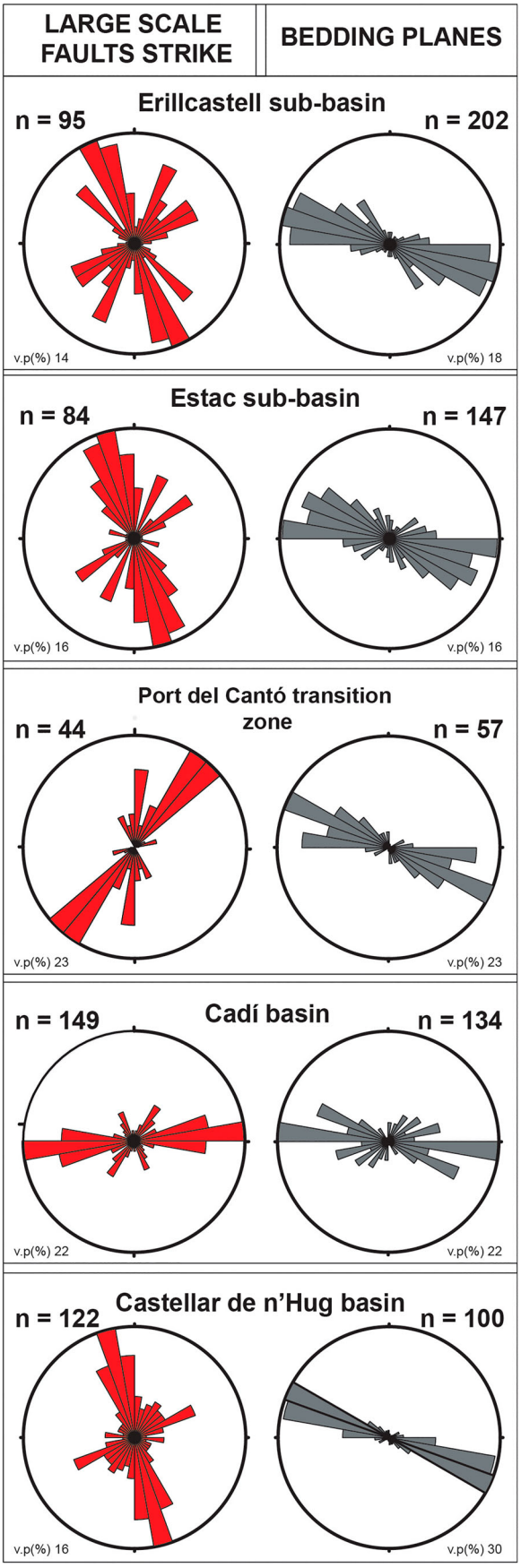

Figure 5. Rose diagrams of the large-scale faults strikes and bedding planes for each basin, sub-basin and for the Port del Cantó transition zone. V.p (%): value in % of total perimeter, *n* = number of faults or bedding planes.

- Lower Red Unit (LRU). It overlies the TU in sedimentary continuity or paraconformity where the GU is mainly composed by large accumulations of volcanic rocks. The LRU is composed of detrital (microconglomerates, sandstones and shales) and volcanic (volcanic tuffs and ignimbrites) rocks.
- Upper Red Unit (URU). This unit always presents an unconformity at its base overlying the previously described units or the pre-Variscan basement rocks. It is formed by detrital (breccias, conglomerates, sandstones and shales) and volcanic (volcanic tuffs and spilitized basalts) rocks.
- Buntsandstein facies (Lower Triassic). This unit presents a basal contact that is often an angular unconformity and rarely a paraconformity. It mainly consists of alternating conglomerates and sandstones, sandstones, and red shales. The latter show intercalations of sandstones at its basal, intermediate and upper part, respectively.
- Muschelkalk facies (Middle Triassic). This unit is composed by limestones, dolostones and marls.
- Keuper facies (Upper Triassic). This unit is composed by shales, gypsum, dolostones and dolerites.

4.2. Structure and cross sections

The study area is located in the southern edge of the Pyrenean Axial Zone. This location has conditioned its overall structure mainly acquired during the Alpine orogeny (Saura & Teixell, 2006). Three cross-sections accompanying the main geological map were elaborated to show the current geometry and the interpretation at depth of the present-day structure of the three basins (Supplementary material). Measured bedding planes (641 planes in total) show an overall azimuth of beds oriented WNW-ESE within the three basins (Figure 5). Besides, an E-W secondary maximum of bedding planes is observed in the three basins, being the main trend in the Cadí basin.

The Erillcastell-Estac basin is cut by several thrust surfaces that are related to forelandward-rotated synformal anticlines known as *têtes-plongeantes* (Séguret, 1972), also observed toward the west (Izquierdo-Llavall et al., 2013). In the Erillcastell sub-basin, the Upper Carboniferous-Permian units are thinner and the number of thrust sheets higher with respect to the Estac sub-basin. In some cases, slaty and pressure-solution cleavage develop in the pelitic and calcareous levels, respectively.

The geological structure admits different interpretations. In cross-sections I and II, we have considered the presence of a basal thrust sheet that could be also reinterpreted as a parautochthonous unit with a disposition similar to that of cross-section III.

The structure of the Cadí and the Castellar de n'Hug basins is simpler in relation to the Erillcastell-Estac basin. The Cadí and Castellar de n'Hug basins present a south-tilted sedimentary succession (average 45°, see cross-section) where major normal faults (also tilted) can be recognized. These faults affect mainly the pre-Variscan basement and the GU. In general, in these two basins these pre-compressional features are better preserved than in the Erillcastell-Estac basin.

The overall tilting of the sedimentary succession allows us to observe fault systems oblique to the main structural trend. The map-scale faults shown in the geological map (Supplementary Material) are distributed in four sets (Figure 5): (i) the NNW-SSE main strike direction is observable in the three basins despite the fact that in the Cadí basin it is minoritary; in the Port del Cantó transition zone, located between the Estac sub-basin and the Cadí basins, this trend is not observed; (ii) the NE-SW to NEE-SWW strike direction is observed in all the basins and it is the main set in the Port del Cantó transition zone; (iii) the E-W strike direction in only observable in the Cadí basin where it is majoritary; (iv) the N-S strike direction is clearly distinguishable in the Port del Cantó transition zone and it is masked by the E-W set in the Estac sub-basin and Castellar de n'Hug basin.

As a whole, fracturing in the South-Pyrenean Late Carboniferous-Permian basins can be interpreted as the result of an E-W to WNW-ESE extension direction that created a conjugate system of normal faults showing a N-S dominant strike. After generalized southward tilting, the east-dipping faults acquired an approximate NE-SW strike whereas the westwards-dipping faults acquired an approximate NW-SE strike. These faults, clearly represented in our map, are significant in basin evolution because they controlled the flow of volcanic and volcaniclastic materials during the Late Carboniferous-Permian times (Simón-Muzás et al., 2022). In addition, the WNW-ESE to W-E set would correspond to the borders of the basins showing Pyrenean direction.

4.3. Basin geometry and synthesis

The presented map gives a 2D image (along an E-W direction) of the Late Carboniferous-Permian-Early Triassic basins of the Eastern Pyrenees and their sedimentary and structural setting. This is an outstanding view, that, in spite of the information missing along the third dimension (in this case, the direction parallel to the dip direction), allows us to extract some interpretations related to the geological evolution of this sector of the Variscan orogen, predating the break-up of Pangea.

In the first place, the thickness of the volcanic and volcaniclastic products in relation to the purely sedimentary series is not disproportionate. Furthermore, the depocenters of the sedimentary and the volcanic filling are often superimposed. These two features suggest that the basins were controlled by tectonic processes rather than by pure volcanic features such as caldera collapses, interpreted in other cases of volcanic subsidence. In the second place, the location of depocenters along the studied area follows a somewhat regular pattern, as shown in the correlation panel accompanying the geological map. The depocenters are regularly spaced and separated by areas where only the red bed units can be recognized. Interestingly, these threshold areas show a lower number of faults oblique or perpendicular to the main trend of the chain, as described in the previous section. Finally, the fault pattern that can be obtained from the map view (supported in some cases by field observations) is consistent with a double fracture system: (i) one of these major systems is parallel to the Pyrenean trend and cannot be directly inferred because of the bias imposed by the outcrop pattern (also parallel to the Pyrenean orientation), (ii) the second one can be determined from the map view (see rose diagrams) and indicates a conjugate system compatible with an approximately E-W extension responsible for thickness changes and the location of the main depocenters along the Pyrenean trend.

5. Conclusions

The detailed geological map of the Upper Carboniferous, Permian and Triassic units along the southern border of the Axial Zone in the Eastern Pyrenees provides an integrated study with unreleased, new information that gives an accurate framework of the tectonic context contemporary with the sedimentation of the Upper Carboniferous-Permian units and their subsequent evolution.

The detailed mapping, accompanied by a stratigraphic correlation panel and three cross sections, permits to define the geometry of the different sub-basins and their arrangement along the southern border of the Axial Zone, thus providing the basis for future basin interpretation. The geological map also provides the clues for analyzing the role of the different structures: faults associated with the basinal period and thrusts linked to the Cenozoic compressional stage. The 641 bedding data measurements complete the structural picture of this large area.

Software

For georeferencing the documents and the elaboration of the final digitized cartography QGIS Desktop 3.30.1 software was used. The geological map was improved by editing the vector file with Inkscape 1.2.2 and 1.3 software versions.

Figures 1–5 were produced with Inkscape 1.2.2 and Inkscape 1.3 software versions.

Geolocation and geographical information

The mapped area is located in the Eastern Pyrenees, between approximate coordinates x: 311,405.292/ y: 4,704,486.924 and x: 430,084.877/ y: 4,676,267.652. We have used ETRS89 as the geodetic reference system with UTM zone 31N, EPSG: 25831.

Coordinates

Erillcastell sub-basin
x_{min} 311834.17
y_{max} 4703427.45
x_{max} 331723.21
y_{min} 4691794.80

Cadí basin
x_{min} 358964.67
y_{max} 4690392.40
x_{max} 395181.45
y_{min} 4683275.26

Estac sub-basin
x_{min} 332424.41
y_{max} 4695265.72
x_{max} 346904.10
y_{min} 4687517.50

Castellar de n'Hug basin
x_{min} 396109.32
y_{max} 4686609.86
x_{max} 429284.259
y_{min} 4679746.84

The Spanish geographic reference information is available at Instituto Geográfico Nacional (IGN) http://centrodedescargas.cnig.es/ BTN200 2014–2018 CC-BY 4.0 ign.es

Acknowledgements

The authors would like to acknowledge the use of Servicio General de Apoyo a la Investigación – SAI, Universidad de Zaragoza that scanned the old maps. Thanks to Maria Jesús Hernández and José A. García Anquela for helping in the elaboration of the cartographies carried out during the 80s. We are grateful to reviewers Carlos Galé, Giedre Beconyte, Michelangelo Martini and the Editor Monica Pondrelli for their careful revision of the manuscript.

Disclosure statement

No potential conflict of interest was reported by the author(s).

Funding

The authors thank the financial support from the projects grants PID2020-114273GB-C22, PID2019-108753GB-C22 and FPU19/02353 funded by MCIN/ AEI/10.13039/ 501100011033, 'ERDF Away of making Europe' and 'ESF Investing in your future'.

Data availability statement

The newly geological map was elaborated based on (1) sketch map of the Late Carboniferous-Permian Cadí basin, scale 1:20,000, (2) the Stratigraphic panel of the Cadí basin and (3) field data elaborated, collected, and presented in the 1981 Josep Gisbert's PhD Thesis entitled 'Estudio Geológico Petrológico del Estefaniense – Pérmico de la Sierra del Cadí. (Pirineo de Lérida): Diagénesis y Sedimentología' available free of charge in his personal ResearchGate profile: https://www.researchgate.net/profile/Josep-Gisbert-Aguilar; (4) Detailed geological map at 1:25,000 scale of the Carboniferous, Permian and Triassic deposits located in the southern border of the Axial Zone in the Eastern Pyrenees with bedding attitude data carried out between 1979 to 1984 elaborated by Josep Gisbert, consulting under request. All the information has been synthesized and presented in the geological map of this publication. Digital elevation models (DEM) to carry out elevation contour lines, nomenclator of population entities and topographic maps databases used to complete the geological map are available in the web http://centrodedescargas.cnig.es/ free of charge for research purposes.

ORCID

Josep Gisbert http://orcid.org/0000-0002-3276-5871
Ana Simón-Muzás http://orcid.org/0000-0001-5824-5367
Antonio Casas-Sainz http://orcid.org/0000-0003-3652-3527
Ruth Soto http://orcid.org/0000-0002-1929-8850

References

Aldega, L., Viola, G., Casas-Sainz, A., Marcén, M., Román-Berdiel, T., & Van der Lelij, R. (2019). Unraveling multiple thermotectonic events accommodated by crustal-scale faults in Northern Iberia, Spain: Insights from K-Ar dating of clay gouges. *Tectonics*, *38*(10), 3629–3651. https://doi.org/10.1029/2019TC005585

Arthaud, F., & Matte, P. (1977). Late Paleozoic strike-slip faulting in southern Europe and northern Africa: Result of a right-lateral shear zone between the Appalachians and the Urals. *Geological Society of America Bulletin*, *88* (9), 1305–1320. https://doi.org/10.1130/0016-7606(1977)88<1305:LPSFIS>2.0.CO;2

Barnolas, A., & Pujalte, V. (2004). La Cordillera Pirenaica. In J. A. Vera (Ed.), *Geología de España* (pp. 233–241). Instituto Geológico y Minero de España.

Choukroune, P., & Séguret, M. (1973). *Carte structurale des Pyrénées, 1/500.000, Université de Montpellier – ELF*. Aquitaine.

Gisbert, J. (1981). *Estudio Geológico – Petrológico del Estefaniense – Pérmico de la Sierra del Cadí (Pirineo de Lérida)*. Diagénesis y Sedimentología [Unpublished PhD, Universidad de Zaragoza], 472 p.

Gisbert, J. (1986). Las Molasas tardihercínicas del Pirineo. In *Geología de España. Libro Jubilar a la memoria de J.M. Ríos* (Vol. 2, pp. 168–184). Madrid: Instituto Geológico y Minero de España.

Izquierdo-Llavall, E., Casas-Sainz, A. M., & Oliva-Urcia, B. (2013). Heterogeneous deformation recorded by magnetic fabrics in the Pyrenean Axial Zone. *Journal of Structural Geology*, *57*, 97–113. https://doi.org/10.1016/j.jsg.2013.10.005

López Berdonces, M. A., Oliván Pociello, C., Oliva Urcia, B., & Pueyo, E. L. (2008). Pyrenean Paleomagnetic databases, VII Congreso Geológico de España. *Geotemas*, *10*, 1219–1222.

López-Gómez, J., Alonso-Azcárate, J., Arche, A., Arribas, J., Barrenechea, J. F., Borruel-Abadía, V., Bourquin, S., Cadenas, P., Cuevas, J., De la Horra, R., Díez, J. B., Escudero-Mozo, M. J., Fernández-Viejo, G., Galán-Abellán, B., Galé, C., Gaspar-Escribano, J., Aguilar, J. G., Gómez-Gras, D., Goy, A., … Viseras, C. (2019). Permian-Triassic rifting stage. In C. Quesada & J. Oliveira (Eds.), *The geology of Iberia: A geodynamic*

approach (pp. 29–112). Regional geology reviews. Springer. https://doi.org/10.1007/978-3-030-11295-0_3

Martí, J. (1986). *El Volcanisme Explosiu Tardihercinià del Pirineu Català* [Unpublished PhD thesis, Universitat de Barcelona]. 304 p.

Martí, J., Solari, L., Casas, J. M., & Chichorro, M. (2019). New late middle to early late Ordovician U–Pb zircon ages of extension-related felsic volcanic rocks in the Eastern Pyrenees (NE Iberia): Tectonic implications. *Geological Magazine*, *156*(10), 1783–1792. https://doi.org/10.1017/S0016756819000116

Mattauer, M. (1968). Les traits structuraux essentiels de la chaîne Pyrénéenne. *Revue de Géographie Physique et Géologie Dynamique*, *10*(1), 3–11.

Muñoz, J. A. (1992). Evolution of a continental collision belt: ECORS-Pyrenees crustal balanced cross-section. In K. R. McClay (Ed.), *Thrust tectonics* (pp. 235–246). Springer.

Porquet, M., Pueyo, E. L., Román-Berdiel, T., Olivier, P., Longares, L. A., Cuevas, J., Ramajo, J., Antolín, B., Aranguren, A., Auréjac, J. B., Bouchez, J. L., Casas, A., Denèle, Y., Gleizes, G., Hilario, A., Izquierdo-Llavall, E., Leblanc, D., Oliva-Urcia, B., Santana, V., … Vegas, N. (2017). Anisotropy of magnetic susceptibility of the Pyrenean granites. *Journal of Maps*, *13*(2), 438–448. https://doi.org/10.1080/17445647.2017.1302364

Puigdefábregas, C. (1975). *La sedimentación molásica en la cuenca de Jaca*. Monografias del Instituto de Estudios Pirenaicos, Pirineos (Jaca), 104, 188 p.

Rodríguez-Méndez, L., Cuevas, J., & Tubía, J. M. (2013). Geological map of the central Pyrenees between the Tena and Aragon valleys (Huesca). *Journal of Maps*, *9*(4), 596–603. https://doi.org/10.1080/17445647.2013.839962

Sanz-López, J. (2004). Silúrico, Devónico y Carbonífero pre- y sin-varisco de los Pirineos. In J. A. Vera (Ed.), *Geología de España* (pp. 250–254). Instituto Geológico y Minero de España.

Saura, E., & Teixell, A. (2006). Inversion of small basins: Effects on structural variations at the leading edge of the Axial Zone antiformal stack (Southern Pyrenees, Spain). *Journal of Structural Geology*, *28*(11), 1909–1920. https://doi.org/10.1016/j.jsg.2006.06.005

Séguret, M. (1972). *Etude tectonique des nappes et séries décollées de la partie centrale du versant sud des Pyrénées*. Série géologie structurale no. 2. Publications de l'Université des Sciences et Techniques du Languedoc (Ustela). 155 p.

Simón-Muzás, A., Casas-Sainz, A. M., Soto, R., Gisbert, J., Román-Berdiel, T., Oliva-Urcia, B., Pueyo, E. L., & Beamud, E. (2022). Axial longitudinal flow in volcanic materials of the Late Carboniferous-Permian Cadí basin (Southern Pyrenees) determined from anisotropy of magnetic susceptibility. *Journal of Volcanology and Geothermal Research*, *421*, Article 107443. https://doi.org/10.1016/j.jvolgeores.2021.107443

Soler i Sampere, M., Henry, J., & Winnock, E. (1972). *Carte géologique des Pyrénées en 4 feuilles*. Feuille N° 4. SNPA. Société Nationale des Pétroles d'Aquitaine. Feuille NK 31-4. Carte de France 1/250000.

Soto, R., Casas-Sainz, A. M., Oliva-Urcia, B., García-Lasanta, C., Izquierdo-Llavall, E., Moussaid, B., Kullberg, J. C., Román-Berdiel, T., Sánchez-Moya, Y., Sopeña, A., Torres-López, S., Villalaín, J. J., El-Ouardi, H., Gil-Peña, I., & Hirt, A. M. (2019). Triassic stretching directions in Iberia and North Africa inferred from magnetic fabrics. *Terra Nova*, *31*(5), 465–478. https://doi.org/10.1111/ter.12416

Ternet, Y., Baudin, T., Laumonier, B., Barnolas, A., Gil Peña, I., & Martin Alfageme, S. (2008). *Mapa Geológico de los Pirineos a E. 1: 400.000*. IGME – BRGM.

Vergés, J., Fernàndez, M., & Martínez, A. (2002). The Pyrenean orogen: Pre-, syn-, and post-collisional evolution. In: Rosenbaum, G. Lister, G. S. 2002. Reconstruction of the evolution of the Alpine-Himalayan orogen. *Journal of the Virtual Explorer*, *8*, 55–74. https://doi.org/10.3809/jvirtex.2002.00058